Polarization analysis of magnetic excitation in multiferroic $Ba_2CoGe_2O_7$

Minoru Soda,[1,2] Lieh-Jeng Chang,[3] Masashige Matsumoto,[4] V. Ovidiu Garlea,[5] Bertrand Roessli,[6] Jonathan S. White,[6] Hazuki Kawano-Furukawa,[1,7] and Takatsugu Masuda[2]

[1]*RIKEN Center for Emergent Matter Science, Wako, Saitama 351-0198, Japan*

[2]*Neutron Science Laboratory, Institute for Solid State Physics, The University of Tokyo, Tokai, Ibaraki 319-1106, Japan*

[3]*Department of Physics, National Cheng Kung University, Tainan 70101, Taiwan*

[4]*Department of Physics, Shizuoka University, Shizuoka 422-8529, Japan*

[5]*Neutron Scattering Division, Oak Ridge National Laboratory, Oak Ridge, Tennessee 37831, USA*

[6]*Laboratory for Neutron Scattering and Imaging, Paul Scherrer Institut, CH-5232 Villigen PSI, Switzerland*

[7]*Department of Physics, Advanced Sciences, G.S.H.S. Ochanomizu University, Tokyo 112-8610, Japan*

(Received 26 April 2018; published 29 June 2018)

Magnetic excitations in the multiferroic $Ba_2CoGe_2O_7$ are measured by combination of unpolarized and polarized neutron-scattering techniques. The unpolarized neutron spectrum reveals an anisotropic $\boldsymbol{Q}$ dependence of the intensity of the electromagnon mode at 4 meV. The analysis of the polarized neutron spectra identifies the directions of the magnetic fluctuations of the observed modes. The determined modes are consistent with the calculation by the extended spin-wave theory. A couple of transverse modes and a single longitudinal mode are involved in the magnetic excitation of $Ba_2CoGe_2O_7$. The longitudinal fluctuation takes on a main role in the electromagnon mode.

DOI: 10.1103/PhysRevB.97.214437

I. INTRODUCTION

In multiferroics, where the ferroelectricity is accompanied by magnetic ordering, coupling between magnetism and dielectricity has been extensively studied [1–4]. The phenomena of a magnetization response with applying an electric field [5–8] and a change of an electric polarization induced by a magnetic field [9–11] are known as the dc magnetoelectric effect. In the dynamics, the hybridization of the spin and the electric polarization waves has attracted great interest [12–15]. The harmonic oscillation of spins can be induced by the electric component of light, and this electric-field active magnon is known as an electromagnon. The multiferroic properties including the electromagnon have been reported in many multiferroics with the cycloidal and proper-screw magnetic structures. Nevertheless multiferroic materials with a collinear structure are rather few [16–18], and åkermanaite compounds $A_2CoB_2O_7$ (A = Ca, Ba; B = Ge, Si) [18–23] are a good playground.

The $Ba_2CoGe_2O_7$ has a two-dimensional square lattice formed by Co^{2+} ions as shown in Fig. 1(a). Co^{2+} ions with spin $S = 3/2$ undergo an antiferromagnetic order with a collinear-magnetic structure below $T_N = 6.7$ K [24,25]. The $Ba_2CoGe_2O_7$ has a multiferroic property [18,26], and the local electric polarization of CoO_4 tetrahedra is explained by the spin-dependent d-p hybridization mechanism [27,28]. The magnetic anisotropy is described in terms of a large single-ion anisotropy D of the easy-plane type and a small spin-nematic interaction J_p, which is equivalent to an interaction of local electric polarizations [20,21]. The spin-nematic interaction realizes the antiferroelectric ground state which relates to the magnetic structure with the easy axis along <100>, as shown in Fig. 1(b). The spin dynamics in $Ba_2CoGe_2O_7$ was studied by inelastic-neutron-scattering (INS) [20,25] and electron-spin-resonance (ESR) [29] measurements. In the neutron study, three modes were observed in the energy-transfer ($\hbar\omega$) region $0 < \hbar\omega < 4$ meV, and one of the observed modes is an optical flat mode, which corresponds to the electromagnon confirmed by electromagnetic wave absorption experiments [19]. In order to explain the observed magnetic excitations, the effective Hamiltonian composed of the conventional bilinear spin interaction $\mathcal{H}_{xxz}$, the single ion anisotropy $\mathcal{H}_D$, a Dzyaloshinskii-Moriya interaction $\mathcal{H}_{DM}$, and a spin-nematic interaction $\mathcal{H}_p$ was analyzed by the extended spin-wave theory [20,30–33]. The INS spectrum was reasonably reproduced by the Hamiltonian, and it was found that the large single-ion anisotropy D was closely related to the electromagnon mode in $Ba_2CoGe_2O_7$. Nevertheless, the detailed scattering function $S(\boldsymbol{q},\omega)$ with the wide-$\boldsymbol{Q}$ region was not clear in the ESR and the previous neutron studies. Furthermore, three modes of the fluctuating magnetic moments are expected in the extended spin-wave theory. The next challenge is to confirm the $S(\boldsymbol{q},\omega)$, including the mode direction in the wide-$\boldsymbol{Q}$ region, and compare it directly with the theoretical study.

In the present paper, we performed the unpolarized and polarized neutron-scattering measurements in $Ba_2CoGe_2O_7$ to analyze the modes of the magnetic excitations. The obtained results are consistent with the calculation by the extended spin-wave theory. The observed magnetic excitations arise due to three types of fluctuations, and the electromagnon around 4 meV contains the longitudinal fluctuation.

II. EXPERIMENTAL DETAILS

The single crystals of $Ba_2CoGe_2O_7$ were grown by the floating-zone method. Unpolarized neutron-scattering measurements were carried out using hybrid spectrometer HYSPEC installed at SNS, Oak Ridge National Laboratory

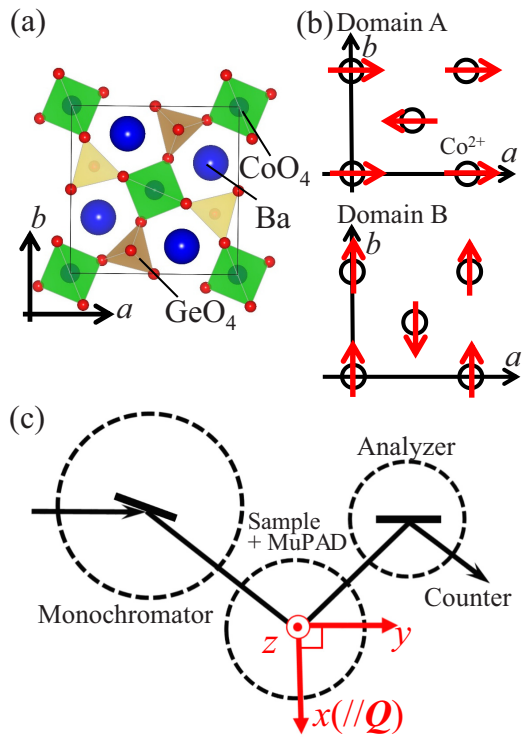

FIG. 1. (a) Schematic crystal structure of $Ba_2CoGe_2O_7$. (b) Schematic magnetic structure of $Ba_2CoGe_2O_7$. (c) Experimental configuration in TASP.

(ORNL), USA [34]. Two experimental conditions with the incident neutron energies of $E_i = 7.5$ and 15 meV were chosen. Polarized neutron-scattering measurements were carried out by combination of the polarization analysis device, MuPAD, and the cold-neutron triple axis spectrometer TASP installed at SINQ, Paul Scherrer Institut (PSI), Switzerland [35]. The final neutron energy E_f was set at 4.66 meV. The neutrons were polarized along the x, y, and z directions as shown in Fig. 1(c); here the x is parallel to the scattering vector $\boldsymbol{Q}$, the z is perpendicular to the scattering plane, and the y is perpendicular to both of the x and z directions. The non-spin-flip (NSF) and spin-flip (SF) scattering cross sections with the neutron spin polarized along the α directions ($\alpha = x, y,$ and z) are described as α-NSF and α-SF scatterings, respectively. The expected components for the NSF and SF scatterings are summarized in Table I, where

$$\sigma_N = \frac{k_f}{k_i}\frac{1}{2\pi\hbar}\int_{-\infty}^{\infty}\langle N(\boldsymbol{Q},0)N^{\dagger}(\boldsymbol{Q},t)\rangle \exp(-i\omega t)dt,$$

$$\sigma_M^{\beta} = \frac{k_f}{k_i}\frac{1}{2\pi\hbar}\int_{-\infty}^{\infty}\langle M^{\beta}(\boldsymbol{Q},0)M^{\beta\dagger}(\boldsymbol{Q},t)\rangle \exp(-i\omega t)dt.$$

TABLE I. The expected components with the neutron spin along the x, y, and z directions.

	NSF	SF
x	σ_N	$\sigma_M^y + \sigma_M^z$
y	$\sigma_N + \sigma_M^y$	σ_M^z
z	$\sigma_N + \sigma_M^z$	σ_M^y

Here $N(\boldsymbol{Q},t)$ is the nuclear structure factor, $M^{\beta}(\boldsymbol{Q},t)$ is a Fourier transform of the β component of the magnetization, and $\beta = x, y,$ and z. In this paper, the magnetic-nuclear interference and the chiral terms were excluded. The flipping ratio of the polarized neutron beam was about 4.9. Throughout this paper, the tetragonal unit cell where the lattice constants are $a = b = 8.410$ Å and $c = 5.537$ Å was used and the scattering plane was the a-c plane. There are magnetic domains of the antiferromagnetic structures with the easy axis along [100] and [010] directions in the tetragonal crystal structure, as shown in Fig. 1(b). The volume ratios of two magnetic domains are assumed to be equal. All measurements were carried out at $T = 1.5$ K by using a liquid-helium cryostat.

III. RESULTS

A. Unpolarized neutron scattering

Figure 2(a) shows the INS spectrum measured at $\boldsymbol{Q} = (H,0,0)$ in the HYSPEC spectrometer with $E_i = 7.5$ meV. Two dispersive excitations at $0 < \hbar\omega < 2.5$ meV and one excitation at 4 meV, which is almost dispersionless, are

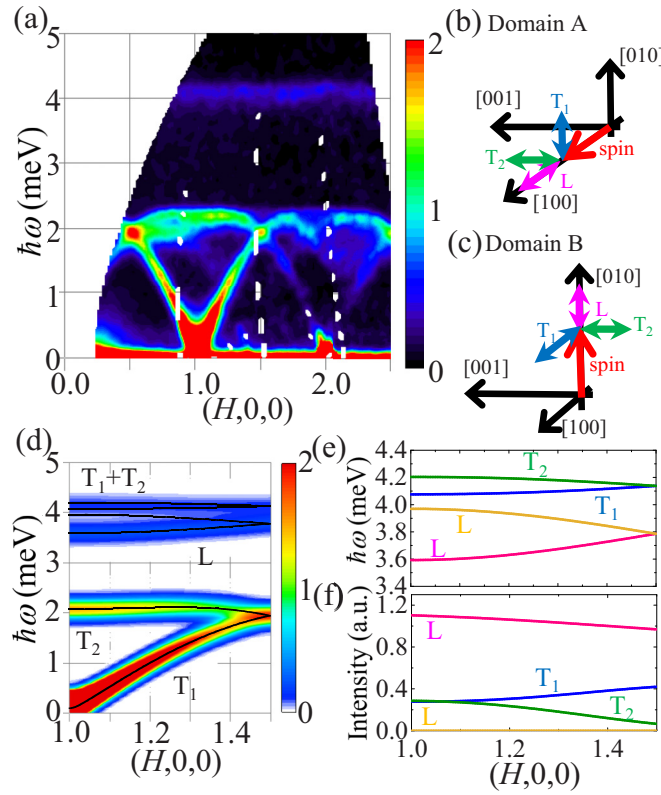

FIG. 2. (a) Inelastic neutron-scattering spectrum obtained by using the HYSPEC spectrometer for $\boldsymbol{Q} = (H,0,0)$. Intensity is indicated by a shade of color. (b,c) Schematics of spin fluctuation for two magnetic domains. Transverse fluctuation in the a-b plane is named the T_1 mode, that along the c direction is named the T_2 mode, and longitudinal fluctuation is named the L mode. (d–f) Magnon calculated by extended spin-wave theory for $\boldsymbol{Q} = (H,0,0)$. (d) Contour map of calculated intensity. Calculated dispersion is shown by the black solid curves. (e,f) Magnon dispersion and intensity at around $\hbar\omega = 4$ meV.

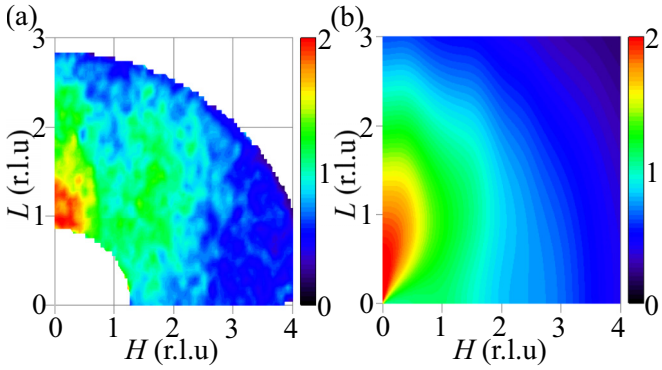

FIG. 3. (a) Neutron-scattering intensity obtained by using the HYSPEC spectrometer in the (H 0 L) plane obtained by integrating the scattering over the energy range 3.5 to 4.5 meV. (b) Intensity calculated by the extended spin-wave theory in the (H 0 L) plane. The calculated intensity is the total one of the T_1, T_2, and L modes.

observed. The spectra are consistent with the previous neutron studies [20,25]. The first branch is the acoustic mode that the excitation energy approaches to zero at (1,0,0). It is noted that the small anisotropy gap was confirmed in the previous study [20]. The second transverse acoustic branch shifted by $\boldsymbol{q} = (1,0,0)$ appears in the spectrum because of two interpenetrating magnetic sublattices. The excitation at 4 meV corresponds to an electromagnon [19].

To investigate the mode around 4 meV, the neutron spectrum was measured in the wide-$\boldsymbol{Q}$ region using $E_i = 15$ meV. Figure 3(a) shows the constant energy cut at $\hbar\omega = 4$ meV for $\boldsymbol{Q} = (H,0,L)$. The neutron intensity monotonically decreases with the increase of the $|\boldsymbol{Q}|$, which is due to the magnetic form factor. In addition it has directional dependence; the intensity along (0,0,L) is larger than that along (H,0,0). This means that the fluctuation of the magnetic moment is anisotropic.

B. Polarized neutron scattering

In order to analyze the modes of the magnetic excitations in detail, the polarized neutron scattering has been carried out at the TASP spectrometer. Figures 4(a), 4(b), and 4(c) show the constant-$\boldsymbol{Q}$ scans at $\boldsymbol{Q} = (1.25,0,0)$ with the neutron spin polarized along x, y, and z directions, respectively. Clear peaks are observed at $\hbar\omega = 1.25$ and 2.25 meV, but the excitation at 4 meV is not clear. In order to make the difference between the NSF and SF intensities at $\hbar\omega = 4$ meV more clear, we count ten times longer time at the energy. To estimate the background intensity, the NSF scatterings at $\hbar\omega = 3$ meV, where no excitation is observed, are measured. Table II shows the neutron intensities at $\hbar\omega = 4$ meV for the signal and

TABLE II. Neutron intensities (counts/8000 kmon.) with the neutron spin along the x, y, and z directions at $\boldsymbol{Q} = (1.25,0,0)$.

	4 meV-NSF	4 meV-SF	3 meV-NSF
x	112	198	102
y	116	183	96
z	178	144	149

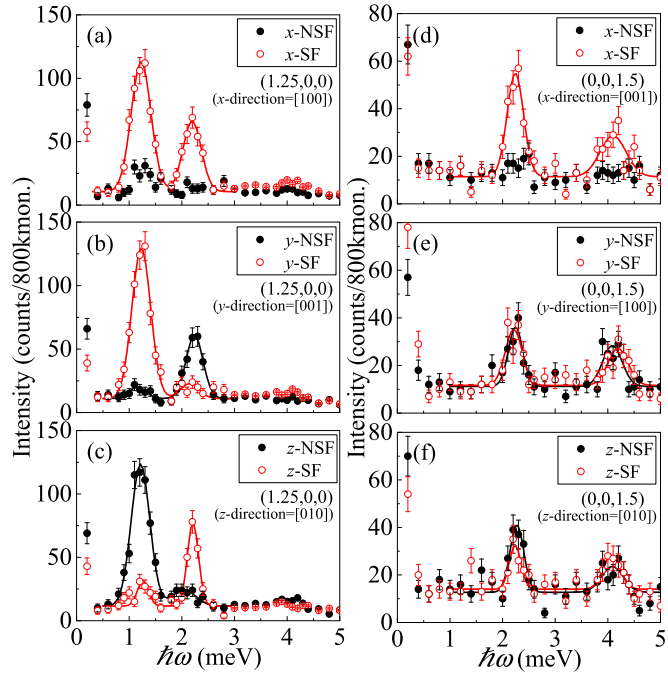

FIG. 4. Typical constant-$\boldsymbol{Q}$ scans obtained by using the TASP spectrometer in PSI. Black closed circles indicate NSF scattering and red opened circles indicate SF scattering. Solid curves are fits to the data by Gaussian functions. (a–c) Constant-$\boldsymbol{Q}$ scans at $\boldsymbol{Q} = (1.25,0,0)$ with the neutron spin along (a) x, (b) y, and (c) z directions. (d–f) Constant-$\boldsymbol{Q}$ scans at $\boldsymbol{Q} = (0,0,1.5)$ with the neutron spin along (d) x, (e) y, and (f) z directions. 800 k monitors correspond to about 520 sec. at $\hbar\omega = 0$.

3 meV for the background. Clear differences were found for all directions of the neutron polarization; x-SF, y-SF, and z-NSF scatterings probe the magnetic excitations, and x-NSF, y-NSF, and z-SF scatterings are at the background level. Data in Figs. 4(a), 4(b), and 4(c) and Table II show that x-SF, y-SF, and z-NSF scatterings probe the excitations at $\hbar\omega = 1.25$ and 4 meV, and x-NSF, y-NSF, and z-SF scatterings probe the excitation at $\hbar\omega = 2.25$ meV. The small peaks at 1.25 meV with the x-NSF, y-NSF, and z-SF scatterings are not intrinsic, which is ascribed to relatively small flipping ratio. Types of the scattering, SF and NSF, for the polarization direction, x, y, and z, for the excitations at 1.25, 2.25, and 4 meV are summarized in Table III.

The constant-$\boldsymbol{Q}$ scans at $\boldsymbol{Q} = (0,0,1.5)$ with the neutron spin polarized along the x, y, and z directions are shown in Figs. 4(d), 4(e), and 4(f), respectively. Clear peaks are observed

TABLE III. The observed scatterings at $\boldsymbol{Q} = (1.25,0,0)$, and the modes allowed in the result of the polarized neutron experiment.

	1.25 meV	2.25 meV	4 meV
x	SF	SF	SF
y	SF	NSF	SF
z	NSF	SF	NSF
Domain A	T_1	T_2	T_1
Domain B	L	T_2	L

at $\hbar\omega = 2.25$ and 4 meV for x-SF, and no peak is observed for x-NSF. In contrast these peaks are observed both for the NSF and SF for the neutron spin polarized along the y and z directions.

IV. DISCUSSION

The spin dynamics in $Ba_2CoGe_2O_7$ is described by the effective spin Hamiltonian

$$\mathcal{H} = \mathcal{H}_{xxz} + \mathcal{H}_D + \mathcal{H}_{\rm DM} + \mathcal{H}_p,$$

as reported in the previous study [20]. Each term is written as

$$\mathcal{H}_{xxz} = \sum_{i,j} \sum_{\alpha=x,y,z} J^\alpha S_i^\alpha S_j^\alpha,$$

$$\mathcal{H}_D = \sum_i D\left(S_i^z\right)^2,$$

$$\mathcal{H}_{\rm DM} = \sum_{i,j} D_{\rm DM}^z(i,j)\left(S_i^x S_j^y - S_i^y S_j^x\right),$$

$$\mathcal{H}_p = -J_p^{\rm eff} \sum_{i,j} O_{XY}(i) O_{XY}(j).$$

Here, S^α is the $S = 3/2$ spin operator, and $O_{XY} = S^X S^Y + S^Y S^X$ is the spin-nematic operator [36,37]. In considering $J^x = J^y = 0.208$ meV, $J^z = 0.253$ meV, $D = 1.034$ meV, $D_{\rm DM}^z = 8.61$ μeV, and $J_p^{\rm eff} = -0.198$ μeV, which were estimated in the previous study [20], the magnon dispersion for $\boldsymbol{Q} = (H,0,0)$ was calculated by the extended spin-wave theory, as shown in Fig. 2(d). The focused dispersions and intensities around $\hbar\omega = 4$ meV are shown in Figs. 2(e) and 2(f), respectively. In this calculation, the magnetic domains of the collinear antiferromagnetic structures with the spins aligned along the [100] (domain A) and [010] (domain B) directions are considered. The calculated modes are classified into three fluctuations: the transverse fluctuation in the a-b plane, the T_1 mode; that in the c direction, the T_2 mode; and the longitudinal fluctuation of the ordered moment, the L mode, as depicted in Figs. 2(b) and 2(c) [20,33]. The acoustic and the optical modes at $0 < \hbar\omega < 2.5$ meV correspond to T_1 and T_2 modes, respectively. On the other hand, the excitation at 4 meV includes the T_1 and T_2 modes with small intensities and the L mode with a large intensity, as shown in Fig. 2(f). The L mode plays a major role in the 4-meV excitation. These T_1, T_2, and L modes are consistent with those identified in the previous ESR studies [29].

The total intensity with T_1, T_2, and L modes around 4 meV is calculated for $\boldsymbol{Q} = (H,0,L)$, as shown in Fig. 3(b). In this calculation, the main intensity is induced by the L mode. Since the magnetic neutron scattering is caused by the component perpendicular to the scattering vector, the L mode, which corresponds to the fluctuation within the c plane, has a large intensity with the scattering vector along the c direction. The directional dependence of the observed intensity in Fig. 3(a) is consistent with the calculation by the extended spin-wave theory.

From the results of the polarized neutron-scattering experiments, we can clarify the direction of the magnetic fluctuation of each mode. Figures 4(a) and 4(d) mean that the observed excitations are induced only by the magnetic scattering because the x-NSF and x-SF scatterings correspond to the nuclear and magnetic ones, respectively, as shown in Table I. Furthermore, we can distinguish the components as either the y and z ones of the fluctuating moment. As for $\boldsymbol{Q} = (1.25,0,0)$, the scattering vector is along [100], which corresponds to the x direction. The y direction is [001], and the z direction is always [010]. It is noted that the z direction is, by convention, the one going out of the scattering plane, which in our case is $(H\ 0\ L)$. The z-NSF scattering probes σ_M^z as in Table I, and in the present coordinate it probes the T_1 mode in domain A in Fig. 2(b) and the L mode in domain B in Fig. 2(c). The z-SF probes the T_2 mode in domains A and B. On the other hand, the y-NSF scattering probes the T_2 mode in domains A and B, and the y-SF probes the T_1 mode in domain A and the L mode in domain B. At $\boldsymbol{Q} = (1.25,0,0)$, thus, the magnetic excitations at 1.25 and 4 meV are induced by the T_1 and/or L modes, while that at 2.25 meV is induced by the T_2 mode. The expected modes for the excitations at 1.25, 2.25, and 4 meV are summarized in Table III.

The observed and calculated intensities for the excitations at 1.25, 2.25, and 4 meV at $\boldsymbol{Q} = (1.25,0,0)$ are summarized in Table IV. Here the observed intensities for the excitations at 1.25 and 2.25 meV are estimated by the Gaussian fits in Figs. 4(a), 4(b), and 4(c). The observed intensities for the excitations at 4 meV are estimated by using the peak intensities in Table II and the energy width at $\boldsymbol{Q} = (0,0,1.5)$ because the profile width at $\boldsymbol{Q} = (1.25,0,0)$ is not clear. The NSF and SF intensities for the excitations at 1.25, 2.25, and 4 meV are quantitatively consistent with the extended spin-wave theory although there is an influence of the small flipping ratio. The neutron intensities of L, T_1, and T_2 modes around 4 meV are 1.05, 0.32, and 0.21, respectively, at $\boldsymbol{Q} = (1.25,0,0)$, as shown in Fig. 2(f), and we can confirm that the observed intensity around 4 meV is mainly from the L mode. Since the intensity ratio of y-SF to y-NSF is estimated to be $(1.37/0.21) \sim 6.5$, the intensity of y-NSF is negligibly small.

TABLE IV. Comparison between the observed intensities and the calculation at $\boldsymbol{Q} = (1.25,0,0)$ and (0,0,1.5). The values in parentheses are estimated by using the present flipping ratio.

	$\boldsymbol{Q} = (1.25,0,0)$						$\boldsymbol{Q} = (0,0,1.5)$			
	1.25 meV		2.25 meV		4 meV		2.25 meV		4 meV	
	Obs.	Cal.	Obs.	Cal.	Obs.	Cal.	Obs.	Cal.	Obs.	Cal.
x-SF	11.34	11.49 (11.49)	5.72	5.36 (5.36)	1.06	1.58 (1.58)	4.01	4.14 (4.14)	2.48	2.28 (2.28)
y-NSF/z-SF	0.85/1.24	0 (2.36)	4.72/4.10	5.36 (5.36)	0.22/0	0.21 (0.49)	2.01/1.21	2.07 (2.50)	1.88/1.36	1.14 (1.37)
y-SF/z-NSF	12.46/11.63	11.49 (11.49)	1.24/1.65	0 (1.10)	0.96/0.32	1.37 (1.41)	2.23/2.19	2.07 (2.50)	1.74/1.33	1.14 (1.37)

The observed modes at $\boldsymbol{Q} = (0,0,1.5)$ are different from those at $\boldsymbol{Q} = (1.25,0,0)$. As for $\boldsymbol{Q} = (0,0,1.5)$, the x direction which corresponds to the scattering vector is along [001], the y direction is [100], and the z direction is [010]. At $\boldsymbol{Q} = (0,0,1.5)$, the y-NSF scattering, which is magnetically equivalent to the z-SF one, probes the L mode in domain A and the T_1 mode in domain B. The y-SF scattering, which is equivalent to the z-NSF one, probes the T_1 mode in domain A and the L mode in domain B. Because of the twinned domains, the NSF and SF scatterings have similar intensities at $\boldsymbol{Q} = (0,0,1.5)$. The observed intensities are estimated by the Gaussian fits in Figs. 4(d), 4(e), and 4(f), and the observed and calculated intensities at $\boldsymbol{Q} = (0,0,1.5)$ are also summarized in Table IV. The magnetic excitation modes determined by the polarized neutron experiment at $\boldsymbol{Q} = (1.25,0,0)$ and $(0,0,1.5)$ are consistent with the predicted modes in the extended spin-wave theory.

The possibility of magnon-phonon coupling is considered in the multiferroics, and the L mode in $Ba_2CoGe_2O_7$ corresponds to the electromagnon [19,33]. In this experiment, however, the magnetic-nuclear interference term, which is induced by the magnon-phonon coupling, could not be studied. If the magnetic-nuclear interference term exists, the y-NSF and z-NSF scatterings should have additional intensities, which correspond to $\langle N \cdot M^{\dagger} \rangle + \langle N^{\dagger} \cdot M \rangle$, besides the scatterings shown in Table I. We could not detect any evidence of the magnon-phonon coupling because no difference between the y-NSF and z-SF or z-NSF and y-SF scatterings could be observed in the present setup. There is also a possibility that another $\boldsymbol{Q}$ position is suitable to observe magnon-phonon coupling. In order to establish the existence of magnon-phonon coupling, an experiment with improved flipping ratio and signal-noise ratio is needed in the future.

V. CONCLUSION

A combination of unpolarized and polarized inelastic neutron-scattering studies has revealed the magnetic excitation modes in the multiferroic $Ba_2CoGe_2O_7$. In the former neutron experiment, the neutron intensity in the wide-$\boldsymbol{Q}$ region was measured. In the latter neutron experiment, the directions of the fluctuating magnetic moments were determined directly. Two excitations with low energy are induced by the two transverse fluctuation modes, and the high-energy excitation which is equivalent to the electromagnon mainly corresponds to the longitudinal fluctuation mode. The obtained results are consistent with the extended spin-wave theory.

ACKNOWLEDGMENTS

The unpolarized neutron experiment was performed by using HYSPEC at SNS/ORNL, USA. The research at ORNL's Spallation Neutron Source was sponsored by the Scientific User Facilities Division, Office of Basic Energy Sciences, U.S. Department of Energy. The polarized neutron experiment was performed by using TASP at SINQ/PSI, Switzerland. Travel expense for the neutron experiment on HYSPEC was supported by the U.S.-Japan collaboration program, and that on TASP was supported by the General User Program for Neutron Scattering Experiments, Institute for Solid State Physics, The University of Tokyo (Proposals No. 13570 and No. 15518). This paper was supported by KAKENHI (Grants No. 15K05123 and No. 17K05516) from the Ministry of Education, Culture, Sports, Science and Technology, Japan.

[1] M. Fiebig, J. Phys. D **38**, R123 (2005).
[2] W. Eerenstein, N. D. Mathur, and J. F. Scott, Nature (London) **442**, 759 (2006).
[3] T. Kimura, Annu. Rev. Mater. Res. **37**, 387 (2007).
[4] S.-W. Cheong and M. Mostovoy, Nat. Mater. **6**, 13 (2007).
[5] Y. Tokunaga, Y. Taguchi, T. Arima, and Y. Tokura, Nat. Phys. **8**, 838 (2012).
[6] Y. Yamasaki, H. Sagayama, T. Goto, M. Matsuura, K. Hirota, T. Arima, and Y. Tokura, Phys. Rev. Lett. **98**, 147204 (2007).
[7] S. Seki, Y. Yamasaki, M. Soda, M. Matsuura, K. Hirota, and Y. Tokura, Phys. Rev. Lett. **100**, 127201 (2008).
[8] M. Soda, K. Kimura, T. Kimura, M. Matsuura, and K. Hirota, J. Phys. Soc. Jpn. **78**, 124703 (2009).
[9] T. Kimura, T. Goto, H. Shintani, K. Ishizaka, T. Arima, and Y. Tokura, Nature (London) **426**, 55 (2003).
[10] M. Soda, K. Kimura, T. Kimura, and K. Hirota, Phys. Rev. B **81**, 100406(R) (2010).
[11] M. Soda, T. Ishikura, H. Nakamura, Y. Wakabayashi, and T. Kimura, Phys. Rev. Lett. **106**, 087201 (2011).
[12] A. Pimenov, A. A. Mukhin, V. Yu. Ivanov, V. D. Travkin, A. M. Balbashov, and A. Loid, Nat. Phys. **2**, 97 (2006).
[13] A. B. Sushkov, R. V. Aguilar, S. Park, S-W. Cheong, and H. D. Drew, Phys. Rev. Lett. **98**, 027202 (2007).
[14] T. Kurumaji, Y. Takahashi, J. Fujioka, R. Masuda, H. Shishikura, S. Ishiwata, and Y. Tokura, Phys. Rev. B **95**, 020405(R) (2017).
[15] M. Mochizuki, N. Furukawa, and N. Nagaosa, Phys. Rev. Lett. **104**, 177206 (2010).
[16] T. Kurumaji, K. Ohgushi, and Y. Tokura, Phys. Rev. B **89**, 195126 (2014).
[17] S. Hayashida, M. Soda, S. Itoh, T. Yokoo, K. Ohgushi, D. Kawana, H. M. Rønnow, and T. Masuda, Phys. Rev. B **92**, 054402 (2015).
[18] H. Murakawa, Y. Onose, S. Miyahara, N. Furukawa, and Y. Tokura, Phys. Rev. Lett. **105**, 137202 (2010).
[19] I. Kézsmárki, N. Kida, H. Murakawa, S. Bordács, Y. Onose, and Y. Tokura, Phys. Rev. Lett. **106**, 057403 (2011).
[20] M. Soda, M. Matsumoto, M. Månsson, S. Ohira-Kawamura, K. Nakajima, R. Shiina, and T. Masuda, Phys. Rev. Lett. **112**, 127205 (2014).
[21] M. Soda, S. Hayashida, B. Roessli, M. Månsson, J. S. White, M. Matsumoto, R. Shiina, and T. Masuda, Phys. Rev. B **94**, 094418 (2016).
[22] M. Akaki, H. Kuwahara, A. Matsuo, K. Kindo, and M. Tokunaga, J. Phys. Soc. Jpn. **83**, 093704 (2014).

[23] M. Soda, S. Hayashida, T. Yoshida, M. Akaki, M. Hagiwara, M. Avdeev, O. Zaharko, and T. Masuda, J. Phys. Soc. Jpn. **86**, 064703 (2017).
[24] T. Sato, T. Masuda, and K. Uchinokura, Physica B **329-333**, 880 (2003).
[25] A. Zheludev, T. Sato, T. Masuda, K. Uchinokura, G. Shirane, and B. Roessli, Phys. Rev. B. **68**, 024428 (2003).
[26] H. T. Yi, Y. J. Choi, S. Lee, and S.-W. Cheong, Appl. Phys. Lett. **92**, 212904 (2008).
[27] C. Jia, S. Onoda, N. Nagaosa, and J. H. Han, Phys. Rev. B **76**, 144424 (2007).
[28] T. Arima, J. Phys. Soc. Jpn. **76**, 073702 (2007).
[29] K. Penc, J. Romhányi, T. Rõõm, U. Nagel, A. Antal, T. Fehér, A. Jánossy, H. Engelkamp, H. Murakawa, Y. Tokura, D. Szaller, S. Bordács, and I. Kézsmárki, Phys. Rev. Lett. **108**, 257203 (2012).
[30] T. Sommer, M. Vojta, and K. W. Becker, Eur. Phys. J. B **23**, 329 (2001).
[31] M. Matsumoto, B. Normand, T. M. Rice, and M. Sigrist, Phys. Rev. Lett. **89**, 077203 (2002).
[32] R. Shiina, H. Shiba, P. Thalmeier, A. Takahashi, and O. Sakai, J. Phys. Soc. Jpn. **72**, 1216 (2003).
[33] M. Matsumoto, M. Soda, and T. Masuda, J. Phys. Soc. Jpn. **82**, 093703 (2013).
[34] B. Winn, U. Filges, V. O. Garlea, M. Graves-Brook, M. Hagen, C. Jiang, M. Kenzelmann, L. Passell, S. M. Shapiro, X. Tong, and I. Zaliznyak, EPJ Web of Conferences **83**, 03017 (2015).
[35] M. Janoschek, S. Klimko, R. Gähler, B. Roessli, and P. Böni, Physica B **397**, 125 (2007).
[36] J. Romhányi, M. Lajkó, and K. Penc, Phys. Rev. B **84**, 224419 (2011).
[37] S. Miyahara and N. Furukawa, J. Phys. Soc. Jpn. **80**, 073708 (2011).